HHS Public Access

Author manuscript

Science. Author manuscript; available in PMC 2017 March 01.

Published in final edited form as:

Science. 2015 May 01; 348(6234): 1253671. doi:10.1126/science.1253671.

Proteomics reveals dynamic assembly of repair complexes during bypass of DNA cross-links

Markus Räschle[1], **Godelieve Smeenk**[2], **Rebecca K. Hansen**[2], **Tikira Temu**[1], **Yasuyoshi Oka**[2], **Marco Y. Hein**[1], **Nagarjuna Nagaraj**[1], **David T. Long**[3], **Johannes C. Walter**[3], **Kay Hofmann**[5], **Zuzana Storchova**[4], **Jürgen Cox**[1], **Simon Bekker-Jensen**[2,*], **Niels Mailand**[2,*], and **Matthias Mann**[1,6,*]

[1]Department of Proteomics and Signal Transduction, Max Planck Institute of Biochemistry, 82152 Martinsried, Germany

[2]Ubiquitin Signaling Group, Department of Disease Biology, Novo Nordisk Foundation Center for Protein Research, University of Copenhagen, DK-2200 Copenhagen, Denmark

[3]Howard Hughes Medical Institute and Department of Biological Chemistry and Molecular Pharmacology, Harvard Medical School, Boston, MA 02115, USA

[4]Maintenance of Genome Stability Group, Max Planck Institute of Biochemistry, 82152 Martinsried, Germany

[5]Institute of Genetics, University of Cologne, 50674 Cologne, Germany

[6]Novo Nordisk Foundation Center for Protein Research, Proteomics Program, University of Copenhagen, DK-2200 Copenhagen, Denmark

Abstract

DNA interstrand cross-links (ICLs) block replication fork progression by inhibiting DNA strand separation. Repair of ICLs requires sequential incisions, translesion DNA synthesis, and homologous recombination, but the full set of factors involved in these transactions remains unknown. We devised a technique called chromatin mass spectrometry (CHROMASS) to study protein recruitment dynamics during perturbed DNA replication in *Xenopus* egg extracts. Using CHROMASS, we systematically monitored protein assembly and disassembly on ICL-containing chromatin. Among numerous prospective DNA repair factors, we identified SLF1 and SLF2, which form a complex with RAD18 and together define a pathway that suppresses genome instability by recruiting the SMC5/6 cohesion complex to DNA lesions. Our study provides a global analysis of an entire DNA repair pathway and reveals the mechanism of SMC5/6 relocalization to damaged DNA in vertebrate cells.

Cellular genomes are particularly susceptible to DNA damage during S phase of the cell cycle, when unrepaired lesions interfere with DNA replication. Several genetically distinguishable pathways have evolved to bypass these roadblocks, involving processing of

*Corresponding author. simon.bekker-jensen@cpr.ku.dk (S.B.-J.); niels.mailand@cpr.kudk (N M); mmann@biochem.mpg.de (M.M.).

Supplementary Materials: www.sciencemag.org/content/348/6234/1253671/suppl/DC1

the stalled replication forks, translesion synthesis (TLS), and homologous recombination (HR) (1–3). Defects in these pathways can lead to genomic rearrangements and cancer predisposition syndromes in higher eukaryotes (3, 4). Among DNA lesions, ICLs are particularly difficult to repair because they affect both strands of the DNA, thereby precluding mechanisms that use an intact complementary strand as a template. Replication of plasmids containing a defined ICL in *Xenopus* egg extracts provided insight into the stepwise bypass of these complex lesions (5). After collision of the replisome with the ICL, the leading-strand DNA polymerase stalls 20 to 40 nucleotides from the cross-link because of steric hindrance by the Mcm2-7 replicative DNA helicase, which unwinds the parental strands ahead of the polymerase. Upon unloading of the helicase and dual incision of one parental strand, leading-strand synthesis advances beyond the ICL. Finally, the incised sister molecule is repaired by HR (6). In agreement with this mechanism, replication-dependent ICL repair in *Xenopus* egg extracts consistently requires the Fanconi anemia protein Fancd2, the Polζ subunit Rev7, and the Rad51 recombinase (5–7). The response to ICL-stalled replication forks also triggers an extensive DNA damage response (DDR) that synchronizes repair status with cell cycle progression and promotes recruitment of the repair machinery. This involves extensive chromatin modifications that serve as docking marks for protein recruitment and change the chromatin architecture to make it permissive for homology-directed repair. However, the factors involved in coordinating all these steps have not yet been defined in an unbiased fashion.

Higher-order chromosome structure is regulated by the SMC (structural maintenance of chromosome) proteins, SMC1 to SMC6 (8). They form heterodimeric complexes involved in sister chromatid cohesion (SMC1/3), chromosome condensation (SMC2/4), and DNA repair (SMC5/6) (9). Like cohesin, the SMC5/6 complex localizes along chromosomes. Local accumulation of SMC5/6 is also observed at DNA double-strand breaks (DSBs) (10) and at stalled replication forks (11, 12), where it regulates the outcome of HR (13). Consistent with this notion, loss of the essential SMC5/6 complex leads to spontaneous chromosomal aberrations and chromosome segregation errors, which are increased strongly by drugs that interfere with DNA replication. In budding and fission yeast, four non-SMC elements (NSE1 to NSE4) stably associate with SMC5/6, conferring ubiquitin and SUMO E3 ligase activity to the complex. In contrast, the NSE5/6 heterodimer only loosely associates with SMC5/6 and appears to be specifically required for its recruitment to DSBs and stalled replication forks (11, 14). So far, no functional orthologs of NSE5/6 have been identified in higher eukaryotes, which raises the question of how the SMC5/6 complex is recruited to DNA lesions in these species.

Dynamic recruitment of DNA repair factors to stalled replication forks

To systematically monitor protein recruitment during ICL repair, we developed chromatin mass spectrometry (CHROMASS) (fig. S1A). In brief, psoralen–cross-linked or undamaged sperm chromatin is replicated in *Xenopus* egg extracts, isolated by sedimentation through a sucrose cushion, and analyzed by a high-performance single-run mass spectrometry workflow (15, 16). Using recently developed algorithms (17), CHROMASS accurately quantifies the recruitment of factors to chromatin. Even at a single time point, as many as 146 known DDR factors were readily detected, 72 of which showed significant enrichment

on the damaged chromatin over the undamaged control [relative change >1.5; false discovery rate (FDR) < 0.05] (Fig. 1A and table S1). Consistent with ICL repair being strictly dependent on replication in this system (5), the recruitment of most DDR factors was sensitive to the replication inhibitor geminin (Fig. 1B and table S1). In total, we analyzed 160 chromatin pellets representing 37 different time points and/or perturbations (fig. S1B). The three independent replicates that we measured for each condition showed a high degree of correlation (median R^2 = 0.92; fig. S2A). Of 5730 quantified proteins, 1349 were specifically enriched on chromatin (fig. S2B and table S1). Intensity profiles of these proteins across all perturbations provide a data-rich resource that can be mined for new insights into chromatin biology.

To analyze the recruitment kinetics of known DNA replication and ICL repair factors, we isolated psoralen–cross-linked chromatin from repair-competent extracts at 15-min intervals. Replication of this damaged template triggered a transient checkpoint response that peaked at 30 min (Fig. 1C), indicating that replication forks reached the ICLs within that time (5, 7). Consistently, most replication initiation and elongation factors peaked early, between 15 and 30 min, whereas most DNA repair factors accumulated only after fork collision with the ICL (Fig. 1D). Concomitant with the unloading of replicative DNA polymerases around 45 min, TLS polymerases (Polκ, Polη, Rev1/3/7), the entire Fanconi core complex, and the Xpf and Fan1 nucleases (18) became enriched on the damaged chromatin. This was followed by the recruitment of the Brca1-A complex, indicating the loading of the HR machinery. Finally, at around 75 min, the Fanci-Fancd2 complex peaked on the chromatin. Given that this complex regulates the incision and TLS step during ICL repair (19, 20), the late peak of Fanci-Fancd2 was surprising. We speculate that this reflects an additional function of the complex, possibly related to the retention of Fancd2 at ultrafine bridges that become visible only in mitosis (21). This global analysis provides detailed insights into the dynamics of protein recruitment to replication forks stalled at ICLs and suggests a highly orchestrated assembly of the repair machinery to ensure a safe handover of potentially dangerous repair intermediates to downstream processes (16).

Identification of damage-specific chromatin binders

Using robust statistical algorithms (22), we next identified for each time point of EXP03-05 (see Fig. 2A and fig. S1B) all proteins with significant enrichment on psoralen–cross-linked chromatin over both undamaged chromatin and a mock control (relative change >1.5; FDR > 0.05). For each protein, we analyzed how often it scored as a damage-specific chromatin binder in the nine evaluated time points (labeled 1 to 9 in Fig. 2A; see also table S1) (16). Only seven proteins were enriched in all nine conditions (Fig. 2B, top bar), whereas the majority of hits scored only in a subset of the analyzed time points. The highest-scoring proteins were almost exclusively known DDR factors. Although the number of identified repair factors increased steadily with decreasing stringency, the overall number of hits increased disproportionately. Therefore, only hits scoring in at least three experimental conditions were included in subsequent analyses. Among the 198 proteins fulfilling these criteria, 87 had previously been implicated in the DDR (red), 17 in sister chromatid cohesion, and 14 in DNA replication (Fig. 2C). The observed maximal damage-specific enrichment of proteins ranged from a factor of 1.5 up to a factor of >400 (Fig. 2D).

To gain further statistical power from these independent experiments (Fig. 2A), we computed a global score for the damage-specific enrichment by means of an FDR-controlled approach (16). Mapping this global score onto a protein-protein interaction network indicated comprehensive coverage of known protein modules implicated in ICL repair (Fig. 2E; see also fig. S3). In contrast, virtually none of the factors involved in unrelated repair pathways—such as nonhomologous end joining, base excision repair, mismatch repair, or postreplicative repair—were robustly enriched on psoralen–cross-linked chromatin. Together with the temporal profiles, these analyses provide a systems-wide proteomic survey of protein recruitment to ICL-stalled replication forks.

To further characterize the damage-specific chromatin binders, we determined whether their recruitment was suppressed in the presence of the replication inhibitor geminin. Although recruitment of the majority of known DDR and replication factors required prior DNA replication, only 24 of the 80 miscellaneous hits showed geminin-sensitive accumulation (Fig. 2, C and E, and figs. S3B and S4). Among these, we identified Ankrd32 and Fam178a, which we refer to as SLF1 and SLF2 (Smc5/6 localization factors 1 and 2), respectively. Both proteins showed prominent enrichment on psoralen–cross-linked chromatin (fig. S3A), and their accumulation peaked together with the early ICL repair factors (see Fig. 1D). Across the entire data set, their intensity profiles clustered most tightly with that of Rad18 (fig. S5). Notably, Rad18, but not its binding partner Rad6 (2, 23), accumulates strongly on cross-linked DNA (Fig. 2E and table S1); this finding suggests that, together with SLF1 and SLF2, RAD18 might play a noncatalytic role in the response to stalled replication forks that is distinct from its RAD6-dependent function as a ubiquitin ligase required for the polymerase switch during postreplicative repair (2).

The RAD18-SLF1-SLF2 complex recruits SMC5/6 to DNA lesions

We next set out to investigate the potential function of SLF1 and SLF2 in the DNA damage response in human cells. Quantitative bacterial artificial chromosome interactomics (QUBIC) (24) confirmed strong and specific interactions among RAD18, SLF1, and SLF2 (Fig. 3, A and B, and fig. S6A). These unbiased experiments also suggested association with components of the SMC5/6 complex. Indeed, when SMC6 was used as bait, RAD18, SLF1, and SLF2 were specifically detected in the pulldowns (Fig. 3A, right, and fig. S6A). Furthermore, the highly abundant RAD6 protein was recovered efficiently in RAD18 but not in SLF2 nor SMC6 pulldowns, and unlike RAD18, neither SLF1, SLF2, nor any components of the SMC5/6 complex were strongly enriched in RAD6 pulldowns (fig. S6B). These findings suggest that RAD18 forms two distinct complexes in HeLa cells: one with RAD6, and another with SLF1 and SLF2 that interacts with the entire SMC5/6 complex in a sub-stoichiometric fashion.

To delineate the molecular nature of the RAD18-SLF1-SLF2-SMC5/6 complex, we confirmed interactions by coimmunoprecipitation. Consistent with work showing that the isolated tandem BRCT repeat of SLF1 recognizes two phosphorylated serine residues located in the C terminus of RAD18 (25), only the wild type, but not mutant RAD18 (S442A/S444A), interacted with full-length SLF1 (Fig. 3C, fig. S6, C to E, and fig. S7). Deletion of the N-terminal tandem BRCT repeat from SLF1 abrogated RAD18 interaction,

although this mutant still bound SLF2 (Fig. 3D). In agreement with a linear organization of the RAD18-SLF1-SLF2-SMC5/6 complex, depletion of SLF1 or SLF2 strongly reduced the amount of SMC5 in RAD18 pulldowns (Fig. 3E). Furthermore, knockdown of SLF1 abolished the interaction between RAD18 and SLF2 (Fig. 3F), whereas depletion of SLF2 did not affect the association of RAD18 with SLF1. We therefore conclude that SLF1 and SLF2 physically link RAD18 to the SMC5/6 complex (Fig. 3G).

To investigate the role of the RAD18-SLF1-SLF2-SMC5/6 complex in the DNA damage response, we asked whether these proteins are physically recruited to laser-induced DNA lesions. Consistent with the accumulation of RAD18 at DSB sites (26) and our physical interaction studies, RAD18, SLF1, SLF2, SMC5, and SMC6 were all recruited to laser-induced DSBs (Fig. 4, A to D, and fig. S8A), as well as to ICLs induced by laser-activated psoralen (fig. S8B). Depletion of SLF1 abolished SLF2 recruitment to DSB sites but not vice versa, further confirming that SLF1 links RAD18 to SLF2 within the complex (Fig. 4D and fig. S8C).

The expression of ectopic SLF1 in cells treated with an SLF1 small interfering RNA (siRNA) targeting the 3′ untranslated region fully restored SLF2 recruitment to laser-induced DNA lesions (Fig. 4E and fig. S8D). Neither SLF1 nor SLF2 depletion impaired RAD18 accumulation at the break sites (Fig. 4D and fig. S8A), but each of these factors was required for SMC5/6 recruitment, further demonstrating the linear relationship among the components of this pathway (Fig. 4, A to D, and fig. S8A).

RAD18 has been shown to accumulate at DSBs via its UBZ domain, which recognizes ubiquity-lation products formed at DNA lesions when RNF8, MDC1, and RNF168 are present (26–29). Consistently, recruitment of RAD18, SLF1, SLF2, and SMC5/6 to microlaser-induced DNA lesions required RNF8, MDC1, and RNF168, but did not require either RAP80 or 53BP1, which function downstream in separate branches of the DSB response (fig. S8, B and D). Likewise, damage recruitment of SLF2 or SMC6 was abolished in cells treated with the proteasome inhibitor MG132, which efficiently depletes the pool of free ubiquitin (30) (fig. S9, C and D). In the *Xenopus* system, depletion of free ubiquitin also abrogated recruitment of all components of the Smc5/6 recruitment cascade, as well as many DNA repair factors known to accumulate at stalled replication forks in a ubiquitin-dependent fashion (Fig. 4F) (31). Because depletion of ubiquitin specifically interferes with early steps of ICL repair without affecting DNA replication (32), these results demonstrate a pivotal role of ubiquitin in the assembly of repair complexes at stalled replication forks.

To further demonstrate how CHROMASS can generate additional insights into chromatin biology via targeted perturbations, we sought to specifically inhibit the HR branch of ICL repair. We added a Brca2-derived peptide (BRC4) to the extract to specifically block the loading of the Rad51 recombinase and formation of recombination intermediates (6). At 90 min, the levels of Rad51 were reduced by a factor of 16 in the presence of BRC4 (Fig. 4G). Recruitment of several Rad51-associated HR factors (Rad51ap1, Rad51c, Xrcc2, Rad54, Mnd1, and Hop2) was similarly reduced. Furthermore, Polη showed a robust decrease, indicating a potential role of this TLS polymerase in HR-associated DNA synthesis. In contrast, addition of the BRC4 peptide did not reveal differential recruitment of enzymes

involved in the processing of recombination intermediates, such as Holliday junction resolvases. Thus, dissolution by the Blm-TopoIIIa-Rmi1-Rmi2 (BTRR) complex, which is recruited early to stalled replication forks by FancM (33), might be the preferred pathway in this system. Our targeted perturbation experiment also demonstrates that the HR branch and the SMC5/6 recruitment cascade are independent pathways.

The SMC5/6 pathway protects cells from replication-associated genotoxic stress

We next examined the impact of compromised RAD18-SLF1-SLF2 function on the maintenance of genome integrity after DNA damage. Depletion of SLF1 or SLF2 increased the sensitivity of U2OS cells to DSB-inducing agents such as ionizing radiation (Fig. 5A and fig. S10A). The degree of hypersensitivity of SLF1- or SLF2-depleted cells to ionizing radiation was comparable to that of cells lacking RNF8 or RNF168 (31, 34), both of which are required for RAD18-SLF1-SLF2 recruitment to DSB sites. In addition, loss of SLF1 or SLF2 function sensitized cells to ionizing radiation to an extent similar to that of RAD18 or SMC6 depletion (Fig. 5A), consistent with the notion that RAD18, SLF1, SLF2, and SMC5/6 function in a linear pathway. Furthermore, depletion of any component of the SMC5/6 recruitment pathway resulted in mild sensitivity to mitomycin C (MMC) (Fig. 5B). Knockdown of RAD18, SLF1, SLF2, or SMC5 enhanced MMC-induced chromosomal aberrations observed in metaphase spreads, comparable to the effect of depleting FANCD2 (Fig. 5C). Ectopic expression of siRNA-insensitive SLF1 in cells treated with SLF1 siRNA significantly reduced MMC-induced chromosomal aberrations (Fig. 5D, asterisks).

The SMC5/6 complex contains a number of non-SMC proteins, collectively referred to as NSE (non-SMC element) proteins (9). Whereas the SMC5/6 and NSE1 to NSE4 subunits are highly conserved across all kingdoms of life, homologs of the NSE5/6 heterodimer have diverged considerably between budding and fission yeast and have not been identified in higher eukaryotes. Using advanced sequence analysis tools (16), we unambiguously found NSE6 to be a member of the SLF2 gene family despite weak overall sequence conservation (fig. S10, B and C). NSE1 to NSE4 are essential proteins in yeast, like SMC5 and SMC6; by contrast, NSE5 and NSE6 appear to promote SMC5/6 complex functions only during genotoxic stress, in particular related to S phase–specific DNA lesions (11, 35). However, deletion of Rqh1 or Mus81 in nse6 or in hypomorphic nse1, nse2, or nse3 mutants results in synthetic lethality, indicating that dissolution and resolution of HR structures becomes critical in cells with compromised SMC5/6 function (35). To test whether this is also the case in human cells, we depleted SMC5/6 pathway proteins from PSNG13 cells, which are unable to dissolve recombination intermediates because of mutations in the BLM helicase (Rqh1 homolog). Depletion of RAD18, SLF1, SLF2, and SMC5 strongly reduced the proliferation of PSNG13 cells relative to BLM-complemented PSNF5 cells (Fig. 5E and fig. S10D). Consistent with an involvement of the SMC5/6 pathway in the resolution of recombination intermediates or the avoidance of illegitimate recombination events (11, 36), knockdown of SLF1 or SLF2 enhanced the rate of sister chromatid exchanges (fig. S10E). Moreover, depletion of SLF1 or SLF2 from U2OS cells significantly increased the frequency of ultrafine bridges and other abnormalities in anaphase cells (fig. S10, F and G, asterisks).

From these lines of evidence, we conclude that SLF1 and SLF2 are important for genome stability maintenance in human cells.

RAD18 facilitates bypass of DNA damage encountered by the replication machinery by promoting the monoubiquitylation of the replication processivity factor PCNA (37). However, we found that both SLF1 and SLF2 were dispensable for replication block–induced PCNA monoubiquitylation and recruitment of the TLS polymerase Polη to stalled replication forks (Fig. 5, G and H). Likewise, knockdown of SLF1 or SLF2 did not affect FANCD2 monoubiquitylation in response to DNA damage (fig. S10H). Thus, we conclude that the RAD18-SLF1-SLF2 complex selectively promotes the function of SMC5/6 in HR, whereas it is not required for RAD18-mediated bypass of replication-blocking lesions.

In addition to the sequence similarity between NSE6 and SLF2 (fig. S10, B and C), we note a considerable analogy between the pathways governing recruitment of the SMC5/6 complex to DNA damage sites in yeast and humans. For instance, Rtt107, a BRCT repeat-containing protein like SLF1, has been shown to mediate SMC5/6 recruitment to DSBs in budding yeast (14). Moreover, the fission yeast ortholog of Rtt107, Brc1, is a high-copy suppressor of SMC5/6 deficiency in a manner requiring a noncatalytic function of RAD18 (38, 39). Given these parallels, we propose that the SMC5/6 recruitment pathway has rapidly evolved to protect cells from replication-associated genotoxic stress.

Combined with existing data, our study suggests that we now know many of the players in postreplicative ICL repair. However, delineating their regulation and potential involvement in related repair pathways remains a challenging task. CHROMASS can be applied to other chromatin-associated processes, and with further development, it offers the perspective to also identify regulatory posttranslational modifications of the chromatin-bound factors in a global manner.

Supplementary Material

Refer to Web version on PubMed Central for supplementary material.

Acknowledgments

We thank A. Hyman and I. Poser for providing BAC cell lines; I. Hickson for providing BLM-deficient and -corrected cells; J. Huang for reagents; J. Cox, F. Gnad, M. Oroshi, R. Scheltema, and C. Schaab for bioinformatics support; S. Schmalbrock, A. Sewo Pires de Campos, C. Kuffer, and A. Kutznetsova for help with microscopy; K. Mayr, I. Paron, G. Sowa, S. Kroiss, B. Splettstösser, and people from the Max Planck animal facility for support; and S. Gruber, B. Pfander, M. Steger, M. Wierer, and F. Coscia for discussion and reading the manuscript Supported by the Center for Integrated Protein Research Munich (CIPSM), the Novo Nordisk Foundation, the Danish Medical Research Council, the Danish Cancer Society, the Lundbeck Foundation, the Bundesministerium für Bildung und Forschung (grant FKZ01GS0861, DiGtoP consortium) and the European Committees Marie Sktodowska-Curie actions (grant PIEF-GA-2012-330675) and 7th Framework Program PROSPECTS (HEALTH-F4-2008-201648). J.C.W. was supported by NIH grant HL098316. J.C.W. is an investigator of the Howard Hughes Medical Institute. The mass spectrometry data have been deposited at Proteome Exchange: http://proteomecentral.proteomexchange.org.

References And Notes

1. Branzei D, Foiani M. Maintaining genome stability at the replication fork. Nat Rev Mol Cell Biol. 2010; 11:208–219. pmid: 20177396. DOI: 10.1038/nrm2852 [PubMed: 20177396]

2. Sale JE. Competition, collaboration and coordination— determining how cells bypass DNA damage. J Cell Sci. 2012; 125:1633–1643. pmid: 22499669. DOI: 10.1242/jcs.094748 [PubMed: 22499669]
3. Deans AJ, West SC. DNA interstrand crosslink repair and cancer. Nat Rev Cancer. 2011; 11:467–480. pmid: 21701511. DOI: 10.1038/nrc3088 [PubMed: 21701511]
4. Jackson SP, Bartek J. The DNA-damage response in human biology and disease. Nature. 2009; 461:1071–1078. pmid: 19847258. DOI: 10.1038/nature08467 [PubMed: 19847258]
5. Räschle M, et al. Mechanism of replication-coupled DNA interstrand crosslink repair. Cell. 2008; 134:969–980. pmid: 18805090. DOI: 10.1016/j.cell.2008.08.030 [PubMed: 18805090]
6. Long DT, Räschle M, Joukov V, Walter JC. Mechanism of RAD51-dependent DNA interstrand cross-link repair. Science. 2011; 333:84–87. pmid: 21719678. DOI: 10.1126/science.1204258 [PubMed: 21719678]
7. Knipscheer P, et al. The Fanconi anemia pathway promotes replication-dependent DNA interstrand cross-link repair. Science. 2009; 326:1698–1701. pmid: 19965384. [PubMed: 19965384]
8. Jeppsson K, Kanno T, Shirahige K, Sjögren C. The maintenance of chromosome structure: Positioning and functioning of SMC complexes. Nat Rev Mol Cell Biol. 2014; 15:601–614. pmid: 25145851. DOI: 10.1038/nrm3857 [PubMed: 25145851]
9. Murray JM, Carr AM. Smc5/6: A link between DNA repair and unidirectional replication? Nat Rev Mol Cell Biol. 2008; 9:177–182. pmid: 18059412. DOI: 10.1038/nrm2309 [PubMed: 18059412]
10. De Piccoli G, et al. Smc5-Smc6 mediate DNA double-strand-break repair by promoting sister-chromatid recombination. Nat Cell Biol. 2006; 8:1032–1034. pmid: 16892052. DOI: 10.1038/ncb1466 [PubMed: 16892052]
11. Bustard DE, et al. During replication stress, non-SMC element 5 (NSE5) is required for Smc5/6 protein complex functionality at stalled forks. J Biol Chem. 2012; 287:11374–11383. pmid: 22303010. DOI: 10.1074/jbc.M111.336263 [PubMed: 22303010]
12. Barlow JH, et al. Identification of early replicating fragile sites that contribute to genome instability. Cell. 2013; 152:620–632. pmid: 23352430. DOI: 10.1016/j.cell.2013.01.006 [PubMed: 23352430]
13. Torres-Rosell J, et al. SMC5 and SMC6 genes are required for the segregation of repetitive chromosome regions. Nat Cell Biol. 2005; 7:412–419. pmid: 15793567. DOI: 10.1038/ncb1239 [PubMed: 15793567]
14. Leung GP, Lee L, Schmidt TI, Shirahige K, Kobor MS. Rtt107 is required for recruitment of the SMC5/6 complex to DNA double strand breaks. J Biol Chem. 2011; 286:26250–26257. pmid: 21642432. DOI: 10.1074/jbc.M111.235200 [PubMed: 21642432]
15. Nagaraj N, et al. System-wide perturbation analysis with nearly complete coverage of the yeast proteome by single-shot ultra HPLC runs on a bench top Orbitrap. Mol Cell Proteomics. 2012; 11:M111.013722. pmid: 24942700. doi: 10.1074/mcp.M113.031591
16. See supplementary materials on *Science* Online.
17. Cox J, et al. Accurate proteome-wide label-free quantification by delayed normalization and maximal peptide ratio extraction, termed MaxLFQ. Mol Cell Proteomics. 2014; 13:2513–2526. pmid: 24942700. DOI: 10.1074/mcp.M113.031591 [PubMed: 24942700]
18. Svendsen JM, et al. Mammalian BTBD12/SLX4 assembles a Holliday junction resolvase and is required for DNA repair. Cell. 2009; 138:63–77. pmid: 19596235. DOI: 10.1016/j.cell.2009.06.030 [PubMed: 19596235]
19. Kratz K, et al. Deficiency of FANCD2-associated nuclease KIAA1018/FAN1 sensitizes cells to interstrand crosslinking agents. Cell. 2010; 142:77–88. pmid: 20603016. DOI: 10.1016/j.cell.2010.06.022 [PubMed: 20603016]
20. MacKay C, et al. Identification of KIAA1018/FAN1, a DNA repair nuclease recruited to DNA damage by monoubiquitinated FANCD2. Cell. 2010; 142:65–76. pmid: 20603015. DOI: 10.1016/j.cell.2010.06.021 [PubMed: 20603015]
21. Chan KL, Palmai-Pallag T, Ying S, Hickson ID. Replication stress induces sister-chromatid bridging at fragile site loci in mitosis. Nat Cell Biol. 2009; 11:753–760. pmid: 19465922. DOI: 10.1038/ncb1882 [PubMed: 19465922]

22. Tusher VG, Tibshirani R, Chu G. Significance analysis of microarrays applied to the ionizing radiation response. Proc Natl Acad Sci USA. 2001; 98:5116–5121. pmid: 11309499. DOI: 10.1073/pnas.091062498 [PubMed: 11309499]

23. Lin JR, Zeman MK, Chen JY, Yee MC, Cimprich KA. SHPRH and HLTF act in a damage-specific manner to coordinate different forms of postreplication repair and prevent mutagenesis. Mol Cell. 2011; 42:237–249. pmid: 21396873. DOI: 10.1016/j.molcel.2011.02.026 [PubMed: 21396873]

24. Hubner NC, et al. Quantitative proteomics combined with BAC TransgeneOmics reveals in vivo protein interactions. J Cell Biol. 2010; 189:739–754. pmid: 20479470. DOI: 10.1083/jcb.200911091 [PubMed: 20479470]

25. Liu T, et al. RAD18-BRCTx interaction is required for efficient repair of UV-induced DNA damage. DNA Repair. 2012; 11:131–138. pmid: 22036607. DOI: 10.1016/j.dnarep.2011.10.012 [PubMed: 22036607]

26. Huang J, et al. RAD18 transmits DNA damage signalling to elicit homologous recombination repair. Nat Cell Biol. 2009; 11:592–603. pmid: 19396164. DOI: 10.1038/ncb1865 [PubMed: 19396164]

27. Panier S, et al. Tandem protein interaction modules organize the ubiquitin-dependent response to DNA double-strand breaks. Mol Cell. 2012; 47:383–395. doi:101016/j.molcel.2012.05.045. pmid: 22742833. [PubMed: 22742833]

28. Helchowski CM, Skow LF, Roberts KH, Chute CL, Canman CE. A small ubiquitin binding domain inhibits ubiquitin-dependent protein recruitment to DNA repair foci. Cell Cycle. 2013; 12:3749–3758. doi:10 4161/cc 26640. pmid: 24107634. [PubMed: 24107634]

29. Bekker-Jensen S, Mailand N. Assembly and function of DNA double-strand break repair foci, in mammalian cells. DNA Repair. 2010; 9:1219–1228. doi:101016/j.dnarep.2010.09.010. pmid: 21035408. [PubMed: 21035408]

30. Dantuma NP, Groothuis TA, Salomons FA, Neefjes J. A dynamic ubiquitin equilibrium couples proteasomal activity to chromatin remodeling. J Cell Biol. 2006; 173:19–26. doi:101083/jcb 200510071. pmid: 16606690. [PubMed: 16606690]

31. Doil C, et al. RNF168 binds and amplifies ubiquitin conjugates on damaged, chromosomes to allow accumulation of repair proteins. Cell. 2009; 136:435–446. doi:101016/j.cell.200812.041. pmid: 19203579. [PubMed: 19203579]

32. Long DT, Joukov V, Budzowska M, Walter JC. BRCA1 promotes unloading of the CMG helicase from a stalled DNA replication fork. Mol Cell. 2014; 56:174–185. doi:101016/j.molcel.2014.08.012. pmid: 25219499. [PubMed: 25219499]

33. Deans AJ, West SC. FANCM connects the genome instability disorders Bloom's syndrome and Fanconi anemia. Mol Cell. 2009; 36:943–953. doi:101016/j.molcel.2009.12.006. pmid: 20064461. [PubMed: 20064461]

34. Mailand N, et al. RNF8 ubiquitylates histones at DNA double-strand breaks and promotes assembly of repair proteins. Cell. 2007; 131:887–900. doi:101016/j.cell.2007.09.040. pmid: 18001824. [PubMed: 18001824]

35. Pebernard S, Wohlschlegel J, Mc Donald WH, Yates JR 3rd, Boddy MN. The Nse5-Nse6 dimer mediates DNA repair roles of the Smc5-Smc6 complex. Mol Cell Biol. 2006; 26:1617–1630. pmid: 16478984. DOI: 10.1128/MCB.26.5.1617-1630.2006 [PubMed: 16478984]

36. Miyabe I, Morishita T, Hishida T, Yonei S, Shinagawa H. Rhp51-dependent recombination intermediates that do not generate checkpoint signal are accumulated in *Schizosaccharomyces pombe* rad60 and smc5/6 mutants after release from replication arrest. Mol Cell Biol. 2006; 26:343–353. pmid: 16354704. DOI: 10.1128/MCB.26.1.343-353.2006 [PubMed: 16354704]

37. Mailand N, Gibbs-Seymour I, Bekker-Jensen S. Regulation of PCNA-protein interactions for genome stability. Nat Rev Mol Cell Biol. 2013; 14:269–282. pmid: 23594953. DOI: 10.1038/nrm3562 [PubMed: 23594953]

38. Sheedy DM, et al. Brc1-mediated DNA repair and damage tolerance. Genetics. 2005; 171:457–468. pmid: 15972456. DOI: 10.1534/genetics.105.044966 [PubMed: 15972456]

39. Lee KM, et al. Brc1-mediated rescue of Smc5/6 deficiency: Requirement for multiple nucleases and a novel Rad18 function. Genetics. 2007; 175:1585–1595. pmid: 17277362. DOI: 10.1534/genetics.106.067801 [PubMed: 17277362]

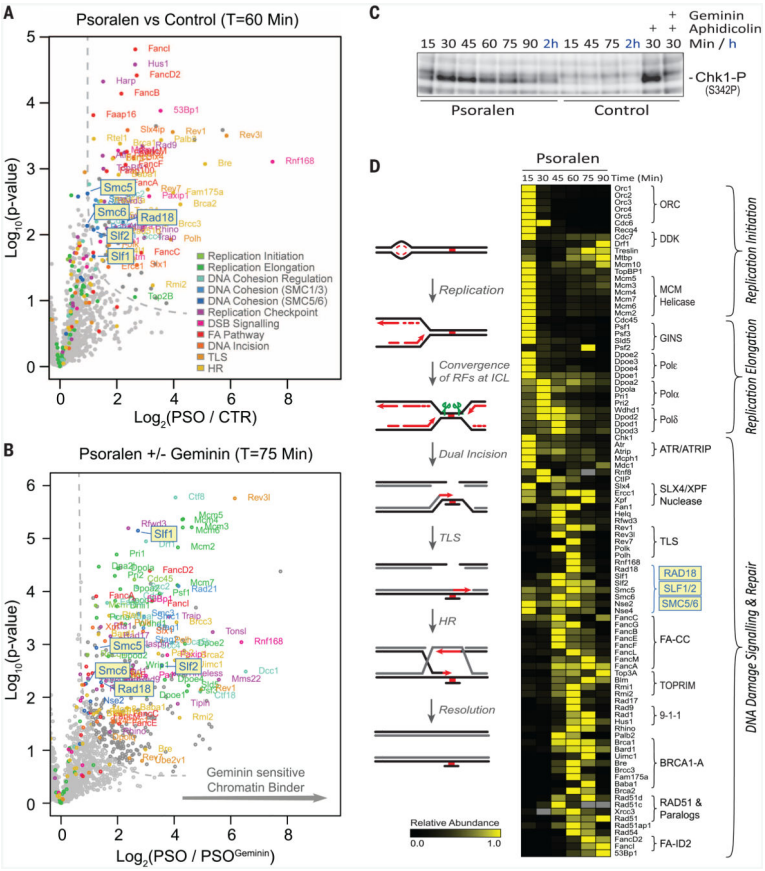

Fig. 1. Dynamic recruitment of proteins to replication forks stalled at psoralen cross-links

Chromatin was replicated in *Xenopus* egg extract and analyzed by CHROMASS. (**A**) Analysis of protein recruitment to psoralen–cross-linked chromatin compared to an undamaged control. The volcano plot shows the mean difference of the protein intensity plotted against the *P* value. Dashed lines indicate the significance cutoff (16). (**B**) Protein recruitment to psoralen–cross-linked chromatin in the presence or absence of the replication inhibitor geminin. (**C**) Analysis of DNA damage checkpoint activation by probing total extracts with antibodies raised against phospho-CHK1. (**D**) CHROMASS analysis of chromatin pellets from the same reactions shown in (C).The heat map shows the relative abundance of the median intensity from three biological replicates calculated for each protein. See table S2 for intensities of all quantified proteins. A model for ICL repair is shown at the left. The same sample was analyzed in (A), (C), and (D).

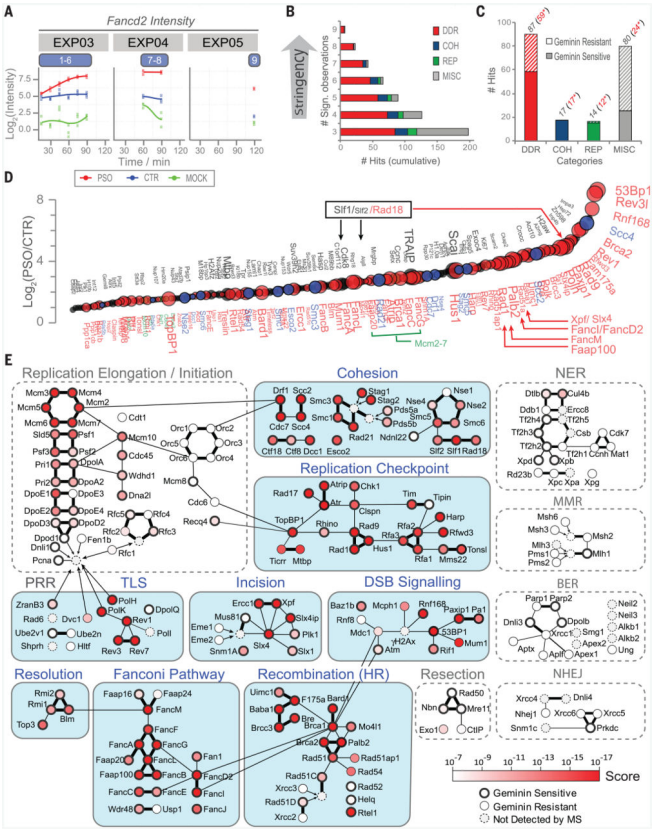

Fig. 2. Pathway analysis reveals comprehensive proteomic coverage of the ICL repair pathway

(**A**) Time points evaluated for the identification of all damage-specific chromatin binders. Representative intensity profile of FancD2 on psoralen–cross-linked chromatin (red), undamaged chromatin (blue), or a mock control lacking chromatin (green) plotted against time. (**B**) The cumulative number of hits in each category plotted against the number of significant observations (table S1), in which a protein was found to be significantly enriched on psoralen–cross-linked chromatin relative to undamaged chromatin and a mock reaction. DDR, DNA damage response; COH, cohesion; REP, DNA replication; MISC, miscellaneous. See table S1 for assignment to categories. (**C**) Replication dependency of damage-specific chromatin binder with at least three significant observations. (**D**) Maximal intensity ratio (PSO/CTR) plotted against the rank of the protein. Dot and label sizes reflect the number of significant observations. (**E**) Mapping a global score for damage-specific enrichment (16) onto a schematic protein interaction network. Low coverage may indicate module members that are not involved in the response to cross-linking agents.

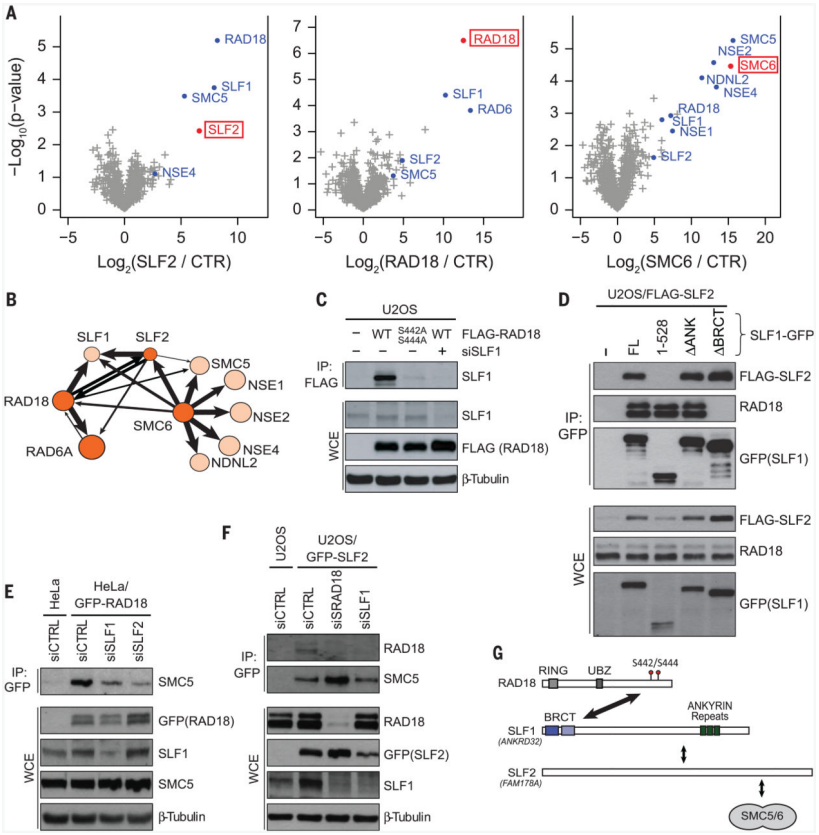

Fig. 3. SLF1 and SLF2 physically link RAD18 to the SMC5/6 complex

(**A**) Green fluorescent protein (GFP) pulldowns from HeLa (BAC) cells expressing SLF2, RAD18, or SMC6 as GFP fusion proteins under their endogenous promoter were analyzed by QUBIC (24). (**B**) Protein interactions identified in (A). Circle size indicates absolute copy number in HeLa cells (see fig. S7C). Baits are shown in dark orange. Arrow size indicates relative intensities of interactors. (**C**) U2OS cells left untreated or transfected with SLF1 siRNA were transfected with indicated FLAG-RAD18 constructs. Whole-cell extracts (WCE) were subjected to FLAG immunoprecipitation (IP) and immunoblotted with antibodies to SLF1, FLAG, and β-tubulin. (**D**) U2OS/FLAG-SLF2 cells were transfected with indicated SLF1 constructs. Interactions among SLF1, SLF2, and RAD18 were analyzed by immunoblotting GFP IPs with the indicated antibodies. (**E**) GFP IPs from HeLa or HeLa/ GFP-RAD18 (BAC) cells transfected with indicated siRNAs were immunoblotted with antibody to SMC5. Knockdown efficiency of the SLF2 siRNA is shown in fig. S6F (**F**) GFP IPs from U2OS cells transfected with the indicated siRNAs, followed by transfection with empty vector or GFP-SLF2 plasmid, were immunoblotted with antibodies to RAD18 and SMC5. (**G**) Schematic depiction of human SLF1 and SLF2 proteins. Conserved BRCT and ankyrin repeat (ANK) domains in SLF1 are highlighted. Interactions among RAD18, SLF1, SLF2, and SMC5/6 are indicated by double-headed arrows.

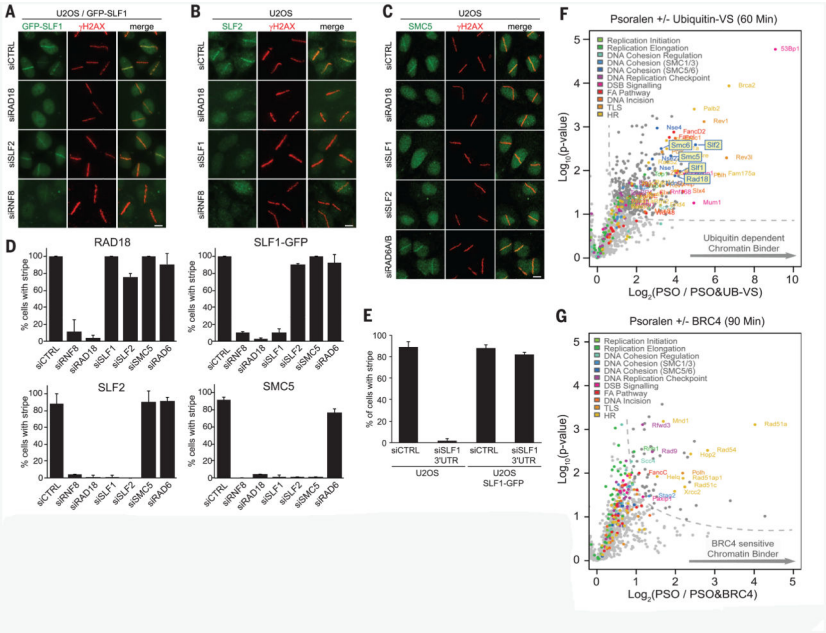

Fig. 4. The RAD18-SLF1-SLF2 complex promotes ubiquitin-dependent recruitment of SMC5/6 to sites of DNA damage

(**A**) U2OS/GFP-SLF1 cells transfected with indicated siRNAs were exposed to laser micro-irradiation, fixed 1 hour later, and immunostained with γ-H2AX antibody. Scale bar, 10 μm. (**B** and **C**) U2OS cells treated as in (A) were coimmunostained with antibody to SLF2 or SMC5, respectively. Scale bar, 10 μm. (**D**) Quantification of data shown in (A) to (C) and fig. S8A. At least 75 cells were counted per data point [mean ± SEM (error bars); $N = 2$]. (**E**) U2OS or U2OS/GFP-SLF1 cells were processed as in (B). At least 100 cells were counted per data point [mean ± SEM (error bars); $N = 2$]. See also fig. S8D. (**F**) CHROMASS analysis of protein recruitment to psoralen–cross-linked chromatin in the presence or absence of ubiquitin vinyl sulfone. (**G**) Protein recruitment to psoralen–cross-linked chromatin in the presence or absence of BRC4 peptide.

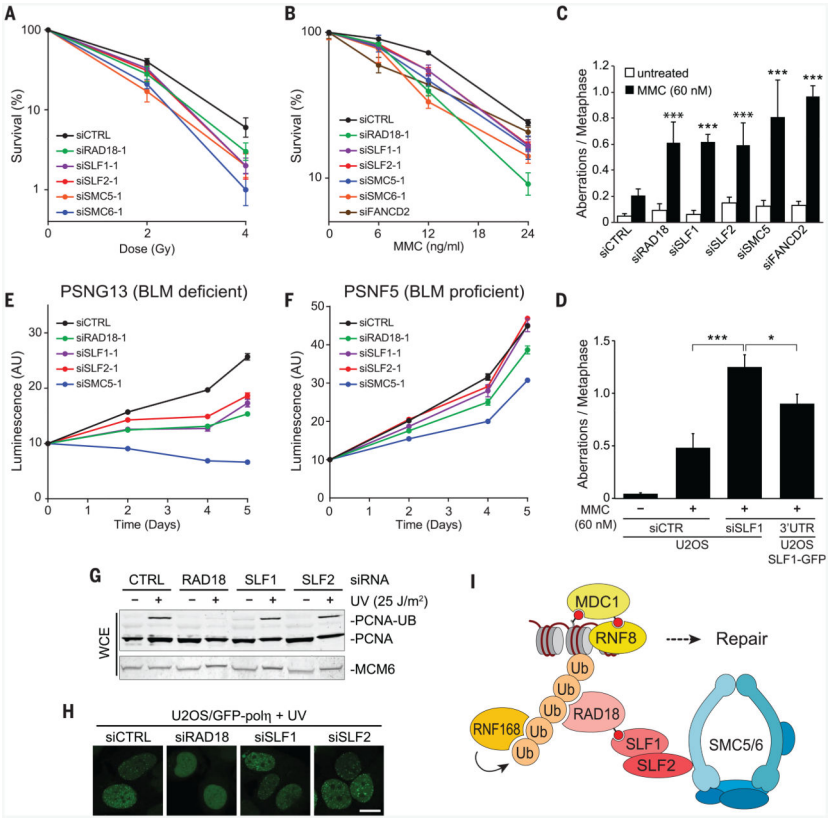

Fig. 5. Role of the RAD18-SLF1-SLF2 complex in genome stability maintenance after DNA damage

(**A**) Clonogenic survival of U2OS cells after exposure to ionizing radiation (mean ± SEM; $N = 3$). See also fig. S10A for an independent set of siRNAs. (**B**) Clonogenic survival of U2OS cells exposed to MMC (mean ± SEM; $N = 3$). (**C**) Chromosomal aberrations of U2OS cells exposed to MMC; 50 metaphases were analyzed per condition (mean ± SD; $N = 2$; $***P < 0.001$, nonparametric t test, all tested against the siCTRL treated with MMC). (**D**) As in (E), except that either U2OS or U2OS/GFP-SLF1 cells were used (mean ± SD; $N = 2$; $***P < 0.001$, $*P < 0.05$, nonparametric t test). (**E** and **F**) Proliferation of PSNG13 or PSNF5 cells (mean ± SD; $N = 3$). See also fig. S10D. (**G**) U2OS were exposed to ultraviolet (UV) irradiation. After 6 hours, extracts were analyzed by immunoblotting with antibodies to PCNA and MCM6. (**H**) U2OS/GFP-polη cells were treated as in (G) and analyzed by confocal microscopy. Scale bar, 10 μm. (I) Model of RAD18-SLF1-SLF2-mediated recruitment of the SMC5/6 complex to damaged DNA.